Polymer 51 (2010) 1320–1327

Contents lists available at ScienceDirect

Polymer

journal homepage: www.elsevier.com/locate/polymer

# Fabrication and characterization of 3-dimensional PLGA nanofiber/microfiber composite scaffolds

Sung Jin Kim [a,1], Da Hyun Jang [b,1], Won Ho Park [a,**], Byung-Moo Min [b,*]

[a] Department of Advanced Organic Materials and Textile System Engineering, and BK21 FTIT, Chungnam National University, Daejeon 305-764, South Korea
[b] Department of Oral Biochemistry and Program of Craniomaxillofacial Reconstruction Science, Dental Research Institute, BK21 CLS, and IBEC, Seoul National University School of Dentistry, 28 Yeonkun-Dong, Chongno-Ku, Seoul 110-749, South Korea

ARTICLE INFO

*Article history:*
Received 7 November 2009
Received in revised form
5 January 2010
Accepted 8 January 2010
Available online 18 January 2010

*Keywords:*
PLGA
Nano-/microfibrous 3-D scaffolds
Normal human epidermal keratinocytes (NHEK)

ABSTRACT

Novel three-dimensional (3-D) nano-/microfibrous poly(lactic-*co*-glycolic acid) (PLGA) scaffolds were fabricated by hybrid electrospinning, involving a combination of solution electrospinning and melt electrospinning. The scaffolds consisted of a randomly oriented structure of PLGA microfibers (average fiber diameter = 28 μm) and PLGA nanofibers (average fiber diameter = 530 nm). From mercury porosimetry, the PLGA nano-/microfiber (10/90) scaffolds were found to have similar pore parameters to the PLGA microfiber scaffolds. PLGA nano-/microfibrous scaffolds were examined and compared with the PLGA microfiber scaffolds in terms of the attachment, spreading and infiltration of normal human epidermal keratinocytes (NHEK) and fibroblasts (NHEF). The cell attachment and spreading of both cell types were several times higher in the nano-/microfiber composite scaffolds than in the microfibrous scaffolds without nanofibers. This shows that the presence of nanofibers enhanced the attachment and spreading of the cells on the nano-/microfiber composite scaffolds. Moreover, the nanofibers helped the cells infiltrate easily into the scaffolds. Overall, this novel nano-/microfiber structures has great potential for the 3-D organization and guidance of cells provided for tissue engineering.



## 1. Introduction

Tissue engineering is a promising approach for providing man-made tissues or organs [1–3]. The design and tailoring of polymer scaffolds is a critical factor for the successful production of man-made tissues because they can be engineered using a combination of cells and polymer scaffolds. In this approach, the cells were incorporated into three-dimensionally structured polymer scaffolds.

Polymer scaffolds play very important roles in tissue engineering by taking on the function of the extracellular matrices (ECM) in the body [4,5]. They are intended to bring cells together and regulate their function, thereby controlling tissue formation and structure. Polymer scaffolds also allow the diffusion of nutrients, metabolites, and soluble factors to enhance tissue formation. Until now, various methods, including particulate-leaching [6], gas forming [7], freeze-drying [8], and phase separation [9], were developed to fabricate porous three-dimensional (3-D) scaffolds from natural and synthetic polymers.

Electrospinning is used widely to fabricate nanofibrous scaffolds from a variety of polymers. The nanofibrous structure is considered to be useful in tissue engineering due to the large surface area that influences the adhesion, migration, and growth of cells [10]. Nanofibrous polymer scaffolds have been examined for tissue engineering of many different types of tissues. Many studies commonly demonstrate that cell attachment, spreading and proliferation were enhanced greatly on these nanofibrous structures [11–15].

However, although a range of nanofibrous scaffolds fabricated by electrospinning have been proposed for tissue engineering, they have limitations for a 3-D culture. Due to the small diameter of the electrospun nanofibers, the fabrication of 3-D scaffolds with a thickness above the millimeter scale remains to be solved. For example, the thickness of human articular cartilage in the knee was observed to range from 0.5 to 7.1 mm [16]. Furthermore, the relatively small pore size compared to the cellular diameter (5–20 μm) could not allow cell migration within the scaffolds [12].

In order to overcome these problems, a few methods for fabricating 3-D nanofibrous structures have been reported [12–14]. Kidoaki et al. [17] attempted multilayering electrospinning to

* Corresponding author. Tel.: +82 2 740 8661; fax: +82 2 740 8665.
** Corresponding author. Tel.: +82 42 821 6613; fax: +82 42 823 3736.
*E-mail addresses:* parkwh@cnu.ac.kr (W.H. Park), bmmin@snu.ac.kr (B.-M. Min).
[1] These authors contributed equally to this work.

0032-3861/$ – see front matter © 2010 Elsevier Ltd. All rights reserved.
doi:10.1016/j.polymer.2010.01.025

create bicomponent scaffolds in which a single component can be removed to generate a porous construct. In addition, electrospinning was combined with salt leaching, which is a well used technique [18]. However, the structural morphology of both fibers and scaffolds might be affected by the leaching out of one component [19]. A second approach is to increase the diameter of the electrospun fibers to ~10 μm by using a higher polymer concentration and/or changing the solvent composition [20]. An increase in fiber diameter increases the porosity of the scaffolds to facilitate cellular infiltration, but may have a negative effect on cell attachment and growth. Finally, a combination of nanofibers and microfibers can be a promising approach for fabricating a 3-D fibrous structure with high porosity. In this approach, nanofibers provide a favorable surface morphology for cell attachment and growth, while microfibers provide the structural environment [19]. Tuzlakoglu et al. [12] fabricated starch/PCL nano-/microfiber scaffolds using a two step process involving fiber bonding and electrospinning. A starch/PCL solution was electrospun to both sides of the starch/PCL microfiber mesh scaffolds. They reported that the cell response changed completely with the addition of nanofibers to the fiber meshes, and osteoblasts covered the scaffolds completely after two weeks of culture. Park et al. [21] fabricated PCL nano-/microfiber scaffolds with a layer-by-layer structure using a two step process involving polymer melt deposition and electrospinning. The results showed that polymer scaffolds with a nanofiber matrice provide favorable conditions for chondrocyte adhesion and proliferation due to the superficial nanotopography in the scaffold. Pham et al. [20] constructed bimodal scaffolds consisting of alternating layers of micro- and nanofibers. This approach is beneficial in that the porosity of scaffolds can be easily varied by controlling the nanofiber/microfiber ratio. However, these 3-D scaffolds have a layered nanofibrous structure in the nano-/microfiber scaffolds from a two step process, instead of a randomly mixed and inter-connected network structure between nanofibers and microfibers. Therefore, the nanofibrous layers, which were formed in sheet-like structures over microfibers, can prevent the cells from infiltrating adequately into the scaffolds.

To fabricate the 3-D scaffolds with a randomly mixed and interconnected network structure between the nanofibers and microfibers, a novel hybrid electrospinning process was designed, combining melt electrospinning with solution electrospinning. When both nano- and microfibers were electrospun simultaneously through two spinnerets, it is important to preclude the electrostatic repulsion or interruption between the two fiber jets. For this, the polymer solution and polymer melt were electrospun simultaneously in opposite directions facing one rotating target, which is called hybrid electrospinning (Fig. 1). This hybrid electrospinning could provide a randomly mixed nano-/microfibrous composite structure with higher pore diameters by simultaneous electrospinning (one-step), as well as a multi-layered nano-/microfibrous composite structure by alternative electrospinning (two- or multi-steps) of solution electrospinning and melt electrospinning. In addition, the thickness of composite scaffolds for 3-D culture could be enlarged to centimeters scale by this hybrid electrospinning. Therefore, the nano-/microfibous composite scaffolds might be adaptable to 3-D culture of various tissues including articular cartilage.

This study investigated the hybrid electrospinning of ploy(D,L-lactide-*co*-glycolide) (PLGA) nano-/microfiber scaffolds. PLGA is a promising tissue engineering material with good biocompatibility and fast biodegradability. The electrospun PLGA nano-/microfiber scaffolds, including pure microfiber PLGA scaffolds for comparison, were characterized in terms of the surface morphology, porosity, their mechanical properties, and cell attachment and in-growth.

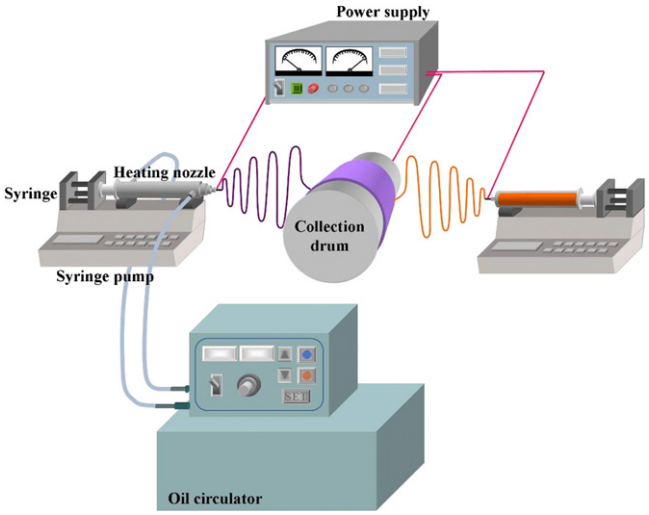


**Fig. 1.** Schematic diagram of the hybrid electrospinning process.

## 2. Materials and methods

### 2.1. Materials

Poly(D,L-lactide-co-glycolide) (PLGA, 50/50) (Mw = 47,000) and 1,1,1,3,3,3, hexafluoro-2-propanol (HFIP) were purchased from PURAC Co. (Holland) and Across (USA), respectively, and used without further purification.

### 2.2. Hybrid electrospinning of PLGA solution and melt

Fig. 1 presents a schematic diagram of the hybrid electrospinning apparatus (Chungpa EMT, Korea) used to fabricate the PLGA nano-/microfiber composite scaffolds. In the hybrid electrospinning process, a spinneret for melt electrospinning was composed of stainless steel capable of oil circulation with a glass syringe placed inside the stainless steel. The temperature of the glass syringe was controlled using an oil circulator with a temperature controller.

In the solution electrospinning compartment, the PLGA nanofibers were prepared by electrospinning a PLGA solution (1–10 wt%) in HFIP. The nanofibers were collected on a target drum placed 8.5 cm from the syringe tip (21G). A voltage of 17.5 kV was applied to the collecting target by a high voltage power supply, and the flow rate of the solution was 6 mL/h. In the melt electrospinning compartment, the PLGA microfibers were prepared by electrospinning a PLGA melt at 210 °C, and were collected on a target drum at a distance of 8 cm from the syringe tip (18 G). A voltage of 17.5 kV was applied to the collecting target using a high voltage power supply and the flow rate of the melt was varied from 1.4 to 5.4 mL/h.

For the PLGA nano-/microfiber composite scaffolds, a PLGA solution (10 wt%) and PLGA melt were electrospun simultaneously in opposite directions facing the rotating target. The compositions (10/90, 20/80, 30/70, wt/wt) of PLGA nano-/microfiber composite scaffold were controlled by adjusting the mass flow rate of the PLGA melt from 1.4 to 5.4 mL/h at a fixed flow rate of the solution (6 mL/h).

As a reference for comparison, the PLGA microfiber scaffold was prepared under the same melt electrospinning conditions at a mass flow rate of 5.4 mL/h.

### 2.3. Characterization

The morphology and pore structure of the electrospun PLGA fibrous scaffolds were observed by a field emission scanning

electron microscopy (FE-SEM, JSM-6335F, JEOL, Japan). Before the observations, platinum was coated by ion sputtering for a few seconds. The average diameter and diameter distribution were obtained by analyzing the SEM images using a custom code image analysis program (Scope Eye II, Korea). The porosity and pore parameters in the inter-fiber region of PLGA fibrous scaffolds were determined using a mercury intrusion technique with an AutoPore III mercury porosimeter (Micromeritics Instrument, Norcross, GA, USA). The mechanical properties of the electrospun PLGA scaffolds were measured using an Instron tensile tester (Instron 8511, Canton, MA, USA). The samples were prepared using the D-638-5 ASTM method and tested at 25 °C and 50% humidity ($n = 10$).

### 2.4. Cells and cell culture

Normal human epidermal keratinocytes (NHEK) were prepared and maintained, as previously described [22,23]. Briefly, the NHEK were isolated from the human foreskins of patients (1–3 years old) undergoing surgery. The epidermal keratinocytes were isolated from separated epithelial tissue by trypsinization, and the primary cultures were established in a keratinocyte growth medium containing 0.15 mM calcium and a supplementary growth-factor bullet kit (KGM; Clonetics, San Diego, CA, USA). The primary NHEK (approximately 70% confluent) were plated at $1 \times 10^5$ cells per 60-mm culture dish and cultured until the cells reached 70% confluence. Second-passage keratinocytes were used in the described experiments. The primary normal human epidermal fibroblasts (NHEF) were established from explant cultures of the foreskin connective tissue, which was excised from a patient undergoing surgery. The cells that proliferated outwardly from the explant culture were cultured continuously in Dulbecco's modified Eagle's medium (DMEM) supplemented with 10% fetal bovine serum (FBS). The assays were performed on the cells in their fourth passage. All the procedures for sampling the human tissue specimens were in accordance with guidelines of the Institutional Review Board (IRB) on Human Subjects Research and Ethics Committee at Seoul National University Dental Hospital, Seoul, Korea.

### 2.5. Cell attachment sssay

Cell attachment was assayed using a modification of the method reported by Mould et al. [24]. Briefly, a PLGA microfiber scaffold and PLGA nano-/microfiber composite scaffold were cut out with a punch (14-mm in diameter) and placed onto 24-well culture plates (Nunc, Danmark). The 24-well culture plates containing the PLGA microfiber scaffold and PLGA nano-/microfiber composite scaffold were soaked in serum-free medium for 1 h at room temperature, followed by rinsing with phosphate-buffered saline (PBS). The cells were detached by a treatment with 0.05% trypsin and 0.53 mM ethylenediaminetetraacetic acid (EDTA) in PBS, resuspended in the culture media ($1 \times 10^5$ cells/500 μl), and then incubated for 1 h at 37°C. The unattached cells were removed by rinsing twice with PBS. The attached cells were fixed with 10% formalin in PBS for 15 min and rinsed twice with PBS. The cells attached to the PLGA scaffolds were stained with hematoxylin and eosin, and the wells were rinsed gently 3 times with double distilled water. The PLGA scaffolds were mounted, and the cells attached to the scaffolds were photographed. In order to ensure a representative count, each scaffold sample was divided into quarters, and two fields per quarter were photographed using an Olympus BX51 microscope at a magnification of 150×.

### 2.6. Scanning electron microscopy

Scanning electron microscopy (SEM) was used to examine the morphological characteristics of the cells cultured onto the PLGA microfiber and PLGA nano-/microfiber scaffolds. The scaffolds were cut out with a punch (14-mm in diameter) and placed onto 24-well culture plates (Nunc, Denmark). The 24-well culture plates containing the PLGA microfiber scaffold and PLGA nano-/microfiber composite scaffold were soaked in serum-free medium for 1 h at room temperature, followed by rinsing with PBS. NHEK and NHEF were detached by a treatment with 0.05% trypsin and 0.53 mM ethylenediaminetetraacetic acid (EDTA) in PBS and resuspended in

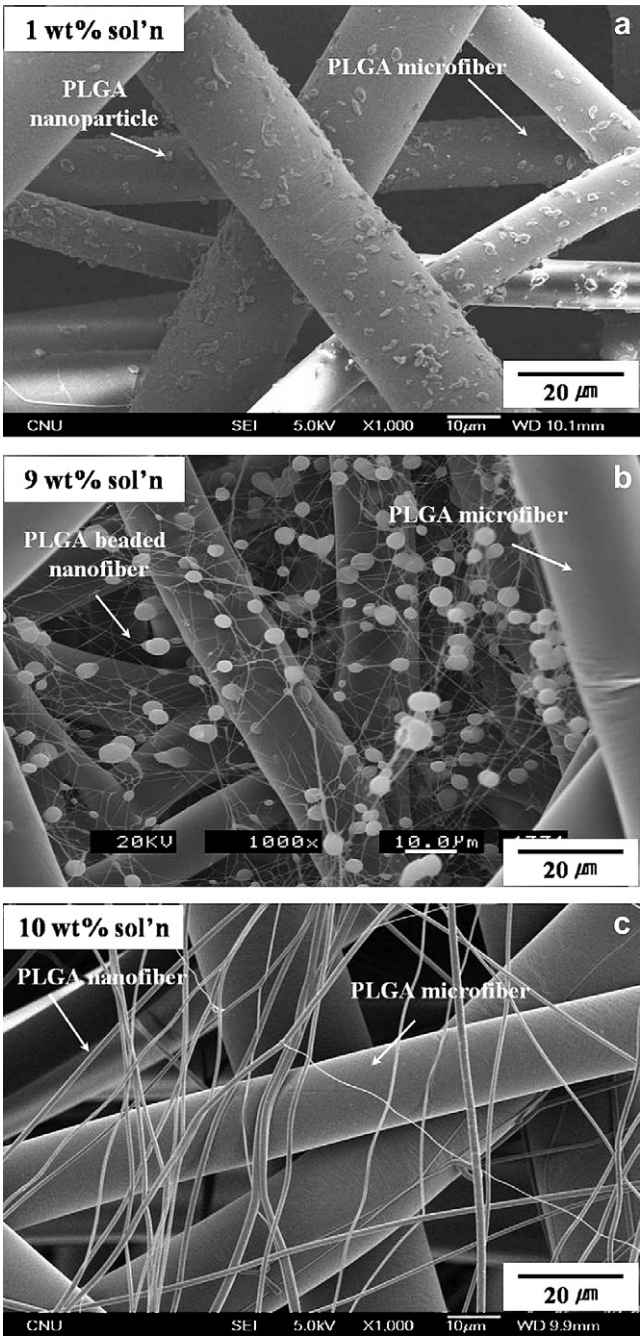


**Fig. 2.** SEM images of the three types of PLGA nano-/microfiber composite scaffolds: (a) nanoparticle/microfiber scaffold, (b) beaded nanofiber/microfiber scaffold, (c) nanofiber/microfiber scaffold.

the culture media ($1 \times 10^5$ cells/500 μl). The cells were plated at $5 \times 10^4$ cells on each matrix and cultured for 1 or 3 days at 37 °C in 5% $CO_2$. The medium was changed every 2 days during the culture period. The bound cells remaining were fixed in 2.5% glutaraldehyde in a 0.1 M cacodylate buffer (pH 7.4) for 10 min. The fixative was then aspirated. After washing in the buffer, the PLGA scaffolds were dehydrated in a graded series of ethanol. After critical point drying (Polaron model 5400; Bio-Rad, Hercules, CA), the samples were sputtered with gold using a SEM coating system (Bio-Rad), and the probes were examined by SEM (JEOL, JSM 840A, Japan). Each scaffold sample was divided into quarters, and four fields per quarter were imaged by SEM at 1000×. The cells that adopted a flattened, polygonal shape with filopodia- and lamellipodia-like extensions were regarded as spreading cells. In contrast, the cells that resisted washing and remained tethered to the scaffold surface were regarded as non-spreading cells.

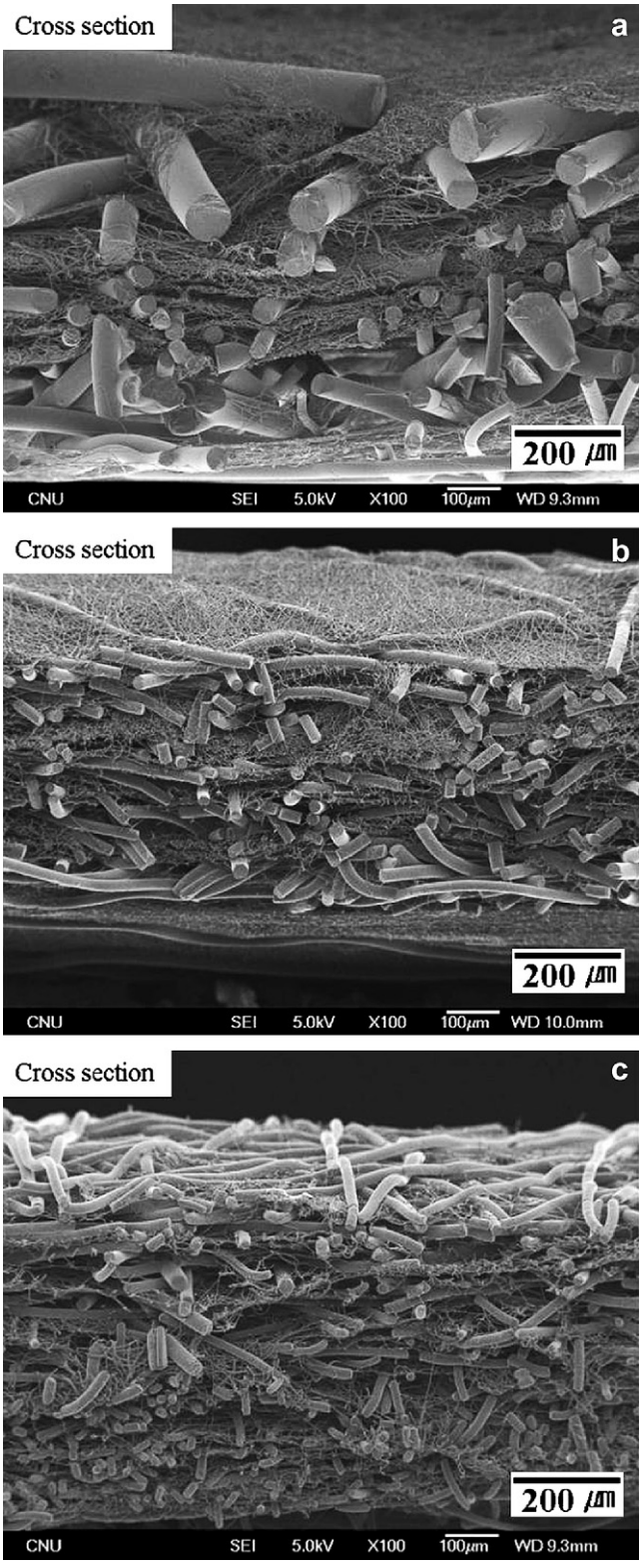


**Fig. 3.** Cross-section SEM images of the PLGA nano-/microfiber composite scaffolds with different nanofiber contents: (a) 10 wt%, (b) 20 wt%, (c) 30 wt%.

### 2.7. Statistics and data analysis

Cell adhesion onto the PLGA scaffolds were compared by an analysis of the variance (ANOVA), using the STATISTICA 6.0 software package. When significant differences were found, pairwise comparisons were performed using a Scheffe's adjustment. *P* values $<0.05$ were considered significant.

## 3. Results and discussion

### 3.1. Morphology of PLGA nano-/microfiber composite scaffolds

The hybrid electrospinning process designed in this study has the advantage in that the nanostructures mixed with microfibers could be varied with the polymer concentration in the solution electrospinning part. Fig. 2 shows SEM images of the nano-/microfiber composite scaffolds fabricated using various PLGA

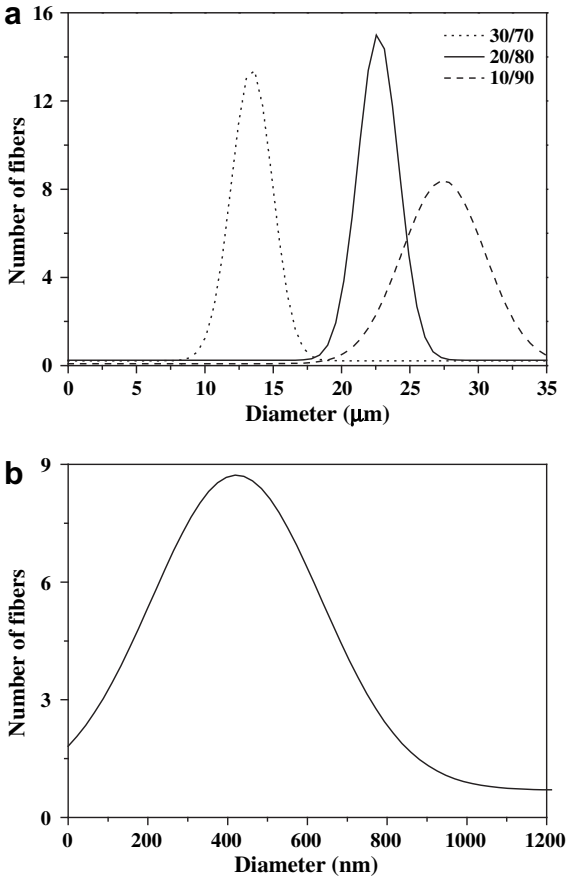


**Fig. 4.** Fiber diameter distributions of the PLGA nano-/microfiber composite scaffolds with different nanofiber contents: (a) microfibers, (b) nanofibers.

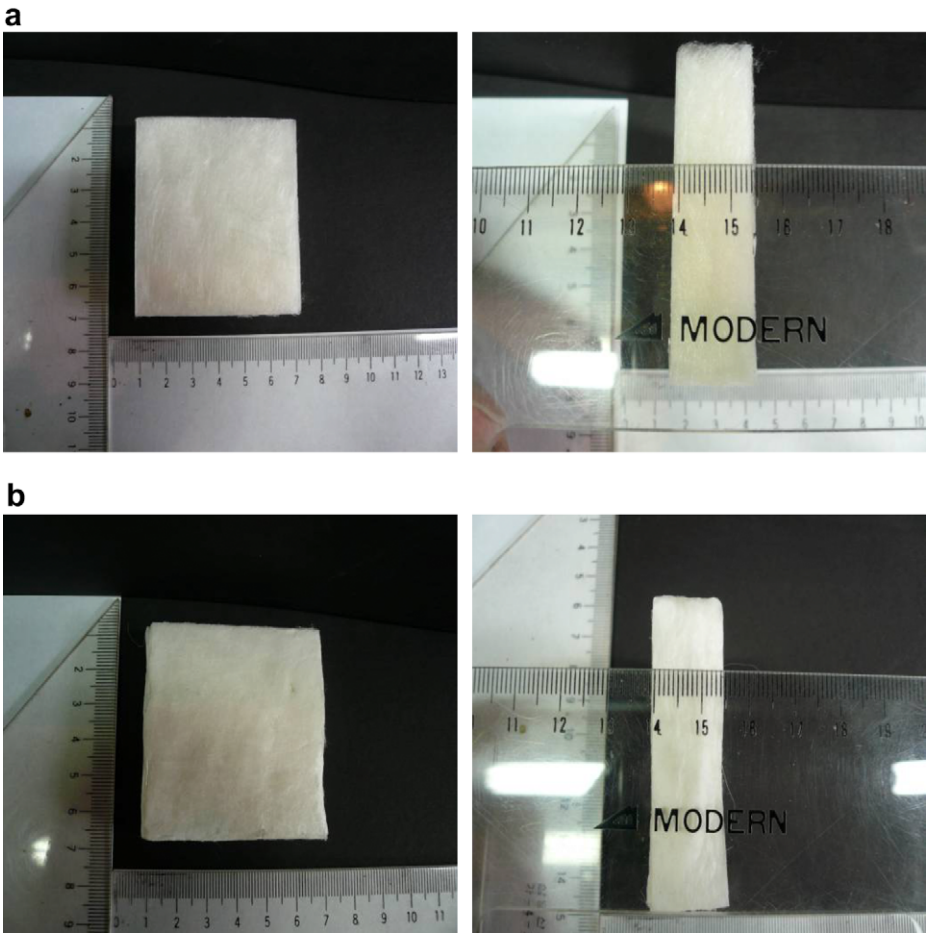


**Fig. 5.** Photographs of (a) PLGA nano-/microfiber (10/90) composite scaffold and (b) PLGA microfiber scaffold.

solutions under fixed melt electrospinning conditions. At lower PLGA concentrations, a nanoparticle/microfiber composite structure with well distributed nanoparticles was observed (Fig. 2a). As the PLGA concentration increased further to 10 wt%, a nanofiber/microfiber composite structure was formed through the beaded nanofiber/microfiber structure (Fig. 2b and c). Therefore, the nanofiber/microfiber composite scaffolds with different microfiber contents were fabricated using a 10 wt% PLGA solution in solution electrospinning compartment. In order to vary the composition of the nanofiber/microfiber composite scaffolds, the change in mass flow rate of the PLGA melt was feasible and desirable because it is difficult to obtain a desired composition of nano-/microfiber scaffolds by changing the flow rate of the polymer solution. Fig. 3 shows cross-section SEM images of the PLGA nano-/microfiber composite scaffolds with different compositions. As shown in Fig. 3, nanofibers and microfibers were mixed randomly and inter-connected, not forming a layered structure, irrespective of the nano-/microfiber composition.

In addition, the diameter of the microfibers in the nano-/microfiber composite scaffolds decreased with increasing the nanofiber content from 10 to 30 wt%. This was attributed to the decrease (from 5.4 to 1.4 mL/h) in mass flow rate of the polymer melt on melt electrospinning. It was reported that the mass flow rate of a polymer melt is the main parameter affecting the diameter of the electrospun fibers in melt electrospinning [25]. This means that the diameter of the electrospun fibers decreases with decreasing the mass flow rate of the polymer melt. Fig. 4 shows the average fiber diameter and its distribution of the PLGA nano-/microfiber composite scaffolds with different compositions. As shown in Fig. 4, the PLGA microfibers in nano-/microfiber composite scaffolds had a larger average diameter from $28.0 \pm 2.6$ μm (10/90) to $14.6 \pm 2.4$ μm (30/70), whereas PLGA nanofibers had a smaller average diameter ($530 \pm 240$ nm). The difference in average fiber diameters between the nanofibers and microfibers was approximately two orders of magnitude.

Electrospinning for longer periods increased the amount of fiber deposition and the thickness of mixed nano-/microfiber scaffolds.

**Table 1**
Porosity and pore parameters of the PLGA microfiber scaffold and PLGA nano-/microfiber (10/90) composite scaffold.

| Sample | TIV (ml/g) | TPA ($m^2$/g) | APD (μm) | *D* (g/ml) | *P* (%) |
|---|---|---|---|---|---|
| PLGA microfiber web | 5.48 | 114.8 | 134.9 | 0.17 | 92.4 |
| PLGA nano-/microfiber (10/90) composite web | 5.40 | 126.1 | 93.9 | 0.17 | 91.2 |

TIV, total intrusion volume; TPA, total pore area; APD, average pore diameter; *D*, bulk density; *P*, porosity.

**Table 2**
Tensile properties of the PLGA microfiber scaffold and PLGA nano-/microfiber (10/90) composite scaffold.

| | Micro 3-D scaffolds | Nano/micro (10/90) 3-D scaffolds | Human Skin |
|---|---|---|---|
| Tensile Strength (Kgf/$mm^2$) | $5.6 \pm 0.7$ | $6.2 \pm 1.0$ | 1.5–15.3 |
| Modulus (Kgf/$mm^2$) | $0.6 \pm 0.1$ | $1.6 \pm 0.6$ | 0.5–3.1 |

Fig. 5 shows representative photographs of the PLGA microfiber scaffolds and nano-/microfiber (10/90) scaffolds with dimensions of 5 × 5 × 1.5 cm. Scaffolds with a thickness up to 2–3 cm could be fabricated by accumulating the mats produced by hybrid electrospinning and melt electrospinning.

### 3.2. Characterization of PLGA nano-/microfiber composite scaffolds

Table 1 summarizes the pore parameters of the PLGA nano-/microfiber (10/90) composite scaffolds determined by mercury porosimetry. The porosity of the PLGA nano-/microfiber (10/90) composite scaffolds was 91.2%, indicating that it is highly porous. The total pore volume was 5.4 mL/g, and the total pore area was 126.1 $m^2$/g. On the other hand, the porosity and pore volume of the PLGA microfiber scaffolds were 92.4% and 5.5 mL/g, respectively, which is similar to those of the PLGA nano-/microfiber (10/90) scaffolds. In particular, the average pore diameter in terms of the volume (V) of the PLGA nano-/microfiber (10/90) composite scaffold and PLGA microfibrous scaffold was 94 μm and 135 μm, respectively. This decrease in pore diameter of the PLGA composite scaffold might be due to the introduction of a small amount of nanofibers (10 wt%). However, a pore size of approximately 100 μm is large enough as to allow the cells to freely migrate in many cases [26].

The pore parameter (pore size, porosity) of the scaffolds is a crucial factor affecting the cell attachment, spreading, and migration. The PLGA nano-/microfiber composite scaffolds with a nanofiber content of 10 wt% had a similar pore parameter to the PLGA microfibrous scaffolds. Therefore, the effect of the nanofibers on cell attachment and spreading on the two PLGA scaffolds (PLGA microfibrous scaffold, PLGA nano-/microfibrous scaffold) with or without a nanofibrous morphology could be examined and compared.

The mechanical properties of the PLGA nano-/microfiber composite scaffold were assessed using a tensile test. The maximum load value of Instron on the PLGA scaffolds was evaluated. Table 2 shows the tensile strength and breaking elongation of the PLGA scaffolds. The PLGA nano-/microfiber composite scaffold had higher tensile strength and elongation at break than the PLGA microfiber scaffolds. This may be explained by the nanofibrous structure entangled with microfibers. The nanofibers in the nano-/microfiber scaffolds can provide higher contacts and/or physical junctions with the microfibers or nanofibers, and thus act as physical crosslinks. In addition, as the PLGA scaffolds possess similar tensile properties to human skin, it was anticipated that PLGA scaffolds would be a suitable tissue engineering scaffold for skin regeneration.

### 3.3. Comparison of cell attachment of NHEK and NHEF of PLGA nano-/microfiber composite scaffold with PLGA microfiber scaffold

Scaffolding materials for tissue engineering approaches are typically designed to promote cell growth and physiological functions, and maintain the normal states of cell differentiation [4]. Two types of 3-D PLGA fibrous scaffolds (microfibrous scaffold and nano-/microfibrous scaffold) were prepared to investigate the effect of the scaffold's nanofibrous structure. PLGA microfibrous scaffold and nano-/microfibrous scaffold contained nanofibers only. This is an important contributing factor for cytocompatibility. Therefore, the presence of a nanofibrous structure in PLGA scaffolds can affect the cellular responses. Since the epidermis and dermis play an important role in reconstructing skin defects, the response of NHEK and NHEF forming this tissue was analyzed *in vitro*. In order to assess and compare cell attachment and in-growth onto PLGA microfiber and nano-/microfiber scaffolds, the cells were seeded onto the PLGA scaffolds without added matrix molecules or BSA.

To observe and compare the biological properties of the PLGA microfiber and nano-/microfiber scaffolds, the cells were seeded onto the microfiber and nano-/microfiber scaffolds that were just soaked in serum-free medium for 1 h. The attachment of cultured NHEK and NHEF was evaluated using a cell attachment assay in serum-free medium. The initial cell attachment onto the PLGA scaffolds were studied because the initial cell attachment and spreading might be important factors in developing wound dressing and scaffolds for tissue engineering. Fig. 6(a) shows representative images of the cells adhered to the PLGA microfiber and nano-/microfiber scaffolds. The attachment of NHEK and NHEF onto the PLGA nano-/microfiber scaffolds increased several times compared to the PLGA microfiber scaffolds (Fig. 6(b)). However, the levels of NHEF attachment on both PLGA microfiber and nano-/microfiber scaffolds were significantly higher than those of the NHEK, respectively. This suggests that the PLGA nano-/microfiber scaffolds are functionally active in terms of cell attachment for both NHEK and NHEF. Therefore, the PLGA nano-/microfiber scaffolds may be suitable as tissue engineering scaffolds for skin regeneration.

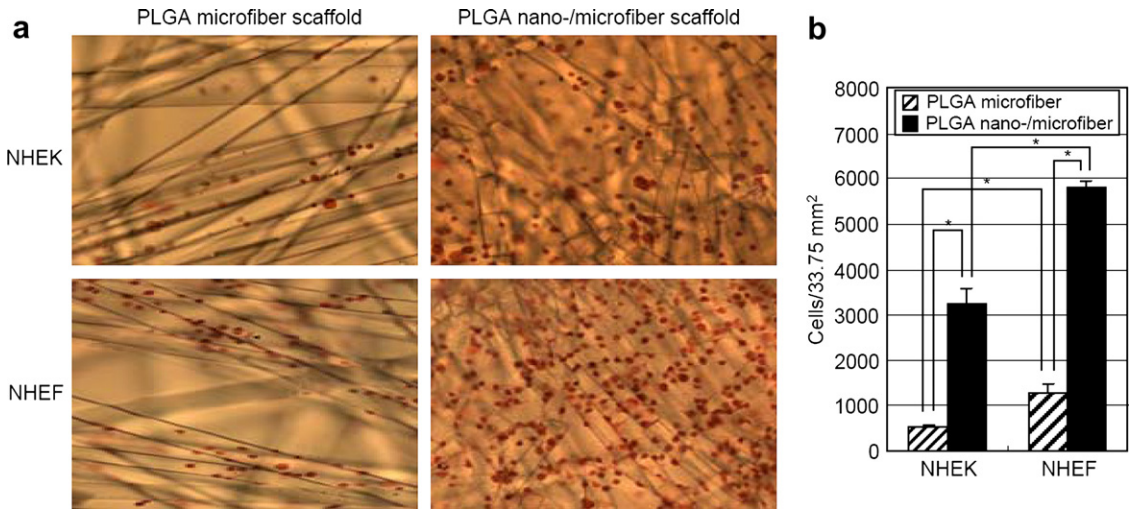


**Fig. 6.** (a) Micrographs and (b) the cell number of NHEK and NHEF adhered to the PLGA nano-/microfiber (10/90) composite scaffold and PLGA microfiber scaffold after 1 h. The data are expressed as the mean ± S.D. ($n = 4$).

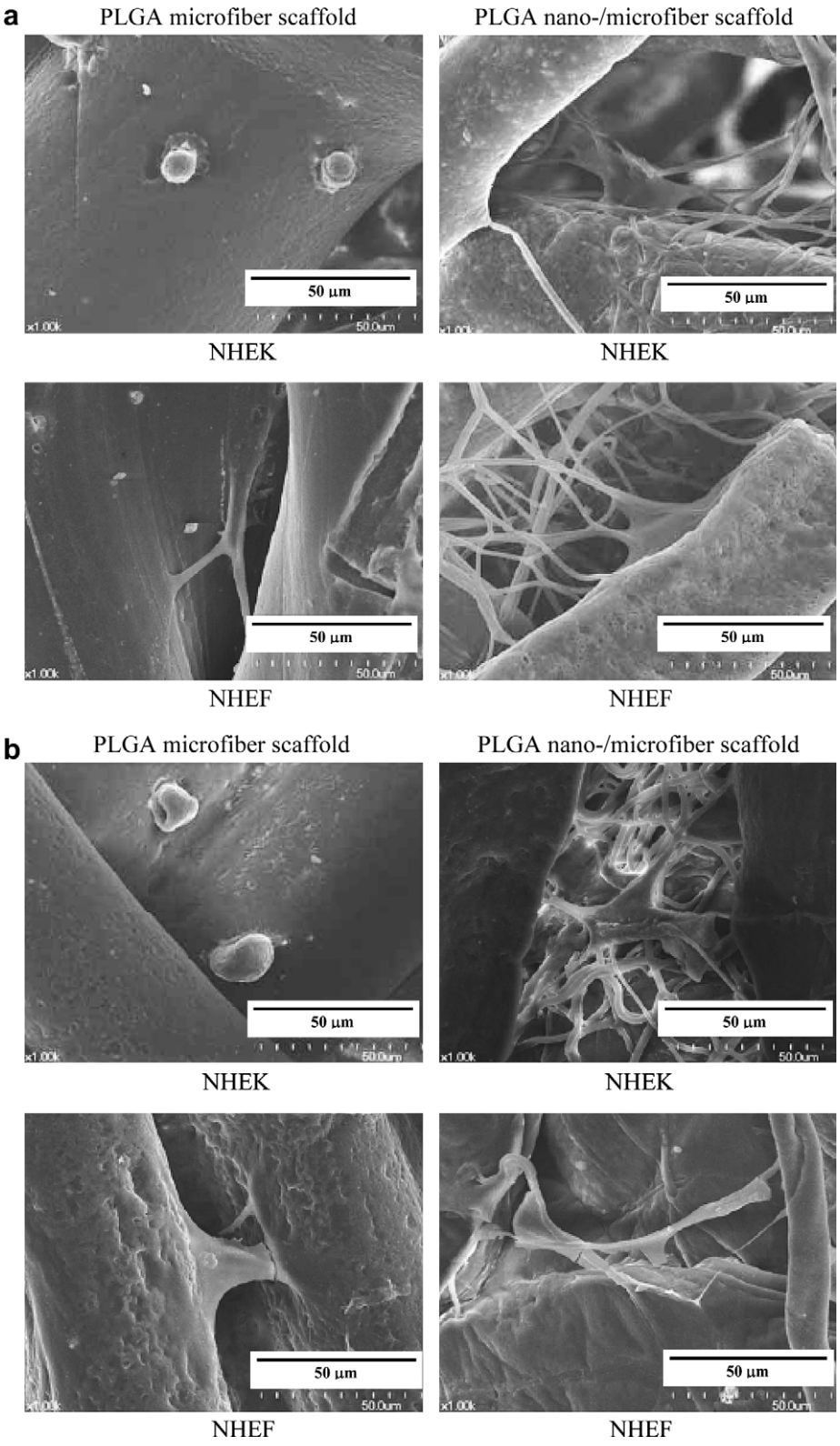


**Fig. 7.** SEM images of cell adhesion and in-growth of NHEK and NHEF to PLGA nano-/microfiber (10/90) composite scaffold and PLGA microfiber scaffold: (a) after 1 day, (b) after 3 days.

### *3.4. Effect of nanofiber in PLGA nano-/microfiber composite scaffolds on cell spreading and infiltration of NHEK and NHEF*

The fabrication of PLGA scaffolds using the hybrid electrospinning process provides a 3-D structure for cell attachment, growth and migration. As described above, the PLGA nano-/microfiber scaffold was functionally active in terms of the initial cell attachment with NHEK and NHEF. We further examined whether the adhered cells were only tethered to the substrate (non-spreading) or spread over the substrate (spreading). Images of

NHEK and NHEF adhered to the PLGA nano-/microfiber scaffolds were taken and used for the spreading assays. Interestingly, cell spreading and infiltration, which was observed on the PLGA nano-/microfiber scaffold, showed a notably different pattern (Fig. 7(a)). NHEK in the PLGA microfiber scaffold did not spread after 1 day, whereas the NHEK were observed deep within the microfibers and partly enmeshed within the nanofibers in the PLGA nano-/microfiber scaffold. NHEF began to enmesh under layers of the PLGA nano-/microfiber scaffold within 1 day. However, the NHEF were bridged between adjacent microfibers in the PLGA microfiber scaffold. Fig. 7(b) shows SEM images of the cellular response to PLGA scaffolds after 3 days. NHEK in the PLGA microfiber scaffold still did not spread, whereas NHEK almost completely covered the microfibers and were fully enmeshed within the nanofibers in the PLGA nano-/microfiber scaffold. The bridge morphology between the microfibers of NHEF was found to be broken, which adversely affected further growth. This shows that a combination of nanofibers with microfibers, particularly a nanofibrous morphology, promotes the interaction between cultured cells and scaffold for the spreading and infiltration of cells. NHEK and NHEF interacted and integrated well with the surrounding PLGA nanofibers and grew in the nanofiber directions, forming a 3-D network of the nano-/microfibrous structure (Fig. 7(b)). Therefore, it is believed that the nanofibrous structure of the scaffolds might play an important role in the attachment, spreading and infiltration of cells.

## 4. Conclusions

In this study, novel 3-D fibrous scaffolds were fabricated to combine the beneficial properties of nanofibers and microfibers. In order to construct the 3-D fibrous scaffolds, a PLGA nano-/microfiber composite scaffold was obtained by hybrid electrospinning, in which both the PLGA solution and PLGA melt produced randomly mixed nanofibers and microfibers, respectively. In addition, PLGA 3-D fibrous scaffolds with a controlled nanofiber content could be fabricated. The mechanical properties of the PLGA microfibrous scaffolds were improved remarkably by introducing a small amount of nanofibers (10 wt%), even though they had similar pore parameters.

In the cytocompatibility assessment for NHEK and NHEF, the PLGA nano-/microfiber composite scaffold promoted cell attachment and in-growth compared to the PLGA microfiber scaffold. This might be due to the nanofibrous topology in the composite scaffold, which is a favorable parameter for cell attachment, growth, and proliferation. The cellular infiltration in nanostructure (fiber, beaded fiber, particle)/microfiber composite scaffolds will be examined in a quantitative manner for long-term cell culture. Finally, a novel 3-D scaffold that combines polymeric microfibers and nanofibers in the composite structure has great potential for skin regeneration.

## Acknowledgments

This study was supported financially by the Biotechnology Development Program (grant number 850-20080090) funded by the Ministry of Education, Science, and Technology (MEST) of Korea.

## References

[1] Khademhosseini A, Langer R, Borenstein J, Vacanti JP. Natl Acad Sci USA 2006;103:2480–7.
[2] Hirano Y, Mooney DJ. Adv Mater 2004;16:17–25.
[3] Griffith LG, Naughton G. Science 2002;295:1009–14.
[4] Lutolf MP, Hubbell JA. Nature Biotechnol 2005;23:47–55.
[5] Liu XH, Ma PX. Ann Biomed Eng 2004;32:477–86.
[6] Mikos AG, Sarakinos G, Leite SM, Vacanti JP, Langer R. Biomaterials 1993;14:323–30.
[7] Shea LD, Smiley E, Bonadio J, Mooney DJ. Nature Biotechnol 1999;17:551–4.
[8] Whang K, Thomas CH, Healy KE, Nuber GA. Polymer 1995;36:837–42.
[9] Nam YS, Park TG. J Biomed Mater Res 1999;47:8–17.
[10] Venugopal J, Ramakrishna S. Appl Biochem Biotechnol 2005;125:147–57.
[11] Min BM, Jeong L, Nam YS, Kim JM, Kim JY, Park WH. Int J Biol Macromol 2004;34:223–30.
[12] Tuzlakogul K, Bolgen N, Salgado AJ, Gomes ME, Piskin E, Reis RL. J Mater Sci Mater Med 2005;16:1099–104.
[13] Li W, Jiang YJ, Tuan RS. Tissue Eng 2006;12:1775–85.
[14] Sun T, Norton D, McKean RJ, Haycock JW, Ryan AJ, MacNeil S. Biotechnol Bioeng 2007;97:1318–28.
[15] Bondar B, Fuchs S, Motta A, Migliaresi C, Kirkpatric CJ. Biomaterials 2008;29:561–72.
[16] Kladny B, Martus P, Schiwy-Bochat KH, Weseloh G, Swoboda B. Int Orthop 1999;23:264–7.
[17] Kidoaki S, Kwon IK, Matsuda T. Biomaterials 2005;26:37–46.
[18] Nam J, Huang Y, Agarwal S, Lannutti J. Tissue Eng 2007;13:2249–57.
[19] Thorvaldsson A, Stenhamre H, Gatenholm P, Walkenstorm P. Biomacromolecules 2008;9:1044–9.
[20] Pham QP, Sharma U, Mikos AG. Biomacromolecules 2006;7:2796–805.
[21] Park SH, Kim TG, Kim HC, Yang DY, Park TG. Acta Biomatialia 2008;4:1198–207.
[22] Min BM, Lee G, Kim SH, Nam YS, Lee TS, Park WH. Bomaterials 2004;25:1289–97.
[23] Min BM, Woo KM, Lee G, Park NH. Exp Cell Res 1999;249:377–85.
[24] Mould AP, Askari JA, Humplhries MJ. J Biol Chem 2000;275:20324–36.
[25] Lyons J, Li C, Ko F. Polymer 2004;45:7597–603.
[26] Telemeco TA, Ayres C, Bowlin GL, Wnek GE, Boland ED, Cohen N, et al. Acta Biomater 2005;1:377–85.